Spin-Circuit Representation of Spin Pumping

Kuntal Roy

Phys. Rev. Applied **8**, 011001 — Published 28 July 2017

DOI: 10.1103/PhysRevApplied.8.011001

Spin-circuit representation of spin pumping

Kuntal Roy*
School of Electrical and Computer Engineering, Purdue University, West Lafayette, Indiana 47907, USA

Circuit theory has been tremendously successful in translating physical equations into circuit elements in organized form for further analysis and proposing creative designs for applications. With the advent of new materials and phenomena in the field of spintronics and nanomagnetics, it is imperative to construct the spin circuit representations for different materials and phenomena. Spin pumping is a phenomenon by which a pure spin current can be injected into the adjacent layers. If the adjacent layer is a material with a high spin orbit coupling, a considerable amount of charge voltage can be generated via inverse spin Hall effect, allowing spin detection. Here we develop the spin circuit representation of spin pumping. We then combine it with the spin circuit representation for the materials having spin Hall effect to show that it reproduces the standard results in literature. We further show how complex multilayers can be analyzed by simply writing a netlist.

According to Onsager's reciprocity [1], spin pumping [2–7] is the reciprocal phenomenon [8] of spin momentum transfer [9], and in this process, unlike charge pumping [10], a precessing magnet [11] injects a *pure* spin current into surrounding conductors. If the adjacent material possesses high spin-orbit coupling [12–15]), a considerable amount of charge voltage can be generated allowing the detection of spin current via inverse spin Hall effect (ISHE) [16–19], which is reciprocal to the direct spin Hall effect (SHE) [20–23].

The expressions of spin current due to spin pumping [4, 5] and spin battery [24, 25] due to a precessing magnetization $\hat{m}$ can be written, respectively as

$$\vec{I}_{SP} = \frac{\hbar}{2e}\left(2G_r^{\uparrow\downarrow}\,\hat{m}\times\frac{d\hat{m}}{dt} + 2G_i^{\uparrow\downarrow}\,\frac{d\hat{m}}{dt}\right) \tag{1}$$

and

$$\vec{V}_{SP} = \frac{\hbar}{2e}\left(\hat{m}\times\frac{d\hat{m}}{dt}\right), \tag{2}$$

where $G^{\uparrow\downarrow}$ $(= G_r^{\uparrow\downarrow} + i\,G_i^{\uparrow\downarrow})$ is the complex (reflection) spin mixing conductance at the ferromagnet-normal metal (FM-NM) interface, which can be determined from microscopic theory [26, 27] and experiments [28]. With scattering formalism, the complex transmission and reflection coefficients are viewed as conductances [26, 29] and when the spin pumping contribution is added to the Landau-Lifshitz-Gilbert (LLG) equation [30] of magnetization dynamics with phenomenological damping parameter [31], the experimentally observable quantities are the enhancement of damping and the ferromagnetic resonance phase shift [4, 5].

Here we construct the spin circuit representation of spin pumping. Kirchoff's circuit laws (current and voltage laws, referred as KCL and KVL, respectively, and they originate from the conservation of charge and energy, respectively) have been ubiquitous in the development of the modern transistor-based technology and there are commercial programs for SPICE (Simulation Program with Integrated Circuit Emphasis), e.g., HSPICE [32]. In this way, an equivalent circuit is constructed based on the underlying physical governing equations for simplified understandings and the development of the complex designs [33]. Such circuit models are general in nature, i.e., they are not limited to semiclassical transport, but also applies to quantum transport [34]. For spintronic circuits, the voltages and currents at different nodes are of 4-components (1 for charge and 3 for spin vector) and the conductances are 4×4 matrices ($c - z - x - y$ basis). Such representations have been developed earlier e.g., for ferromagnet (FM), normal metal (NM), FM-NM interface, spin Hall effect (SHE) [25, 35, 36].

Since spin pumping injects *pure* spin current (without the charge component), we deduce the 3-component version and show that it can reproduce the established expressions in literature for effective spin mixing conductance considering *diffusive* NM [5] and the inverse spin Hall voltage due to spin pumping [14], utilizing *semiclassical* models. We further employ such spin circuit for a complex structure of multilayers [37] and show that it simply reduces to an equivalent circuit *without* invoking any boundary condition and matches the mathematically derived expression in literature [38]. We show how to write a simple netlist to solve and derive the effective spin mixing conductance for complex structures [37]. We can simply write a netlist containing the conductances and voltage/current sources to solve for the voltages/currents at the different nodes using a circuit solver. For more complex multilayers, the analytical expression becomes tedious and this depicts the prowess of the spin circuit approach.

Figure 1 shows the spin circuit representation of spin pumping that constitutes the spin circuit representations of FM module, NM module, and FM-NM interface. The NM module can possess spin Hall effect and the inverse spin Hall charge voltage can be generated due to spin pumping, which will be addressed later in Fig. 2. The conductances [29] (after the necessary modifications [25, 35]) and spin voltage sources in Figure 1 are represented as follows.

* royk@purdue.edu, kuntalroy@gmail.com.

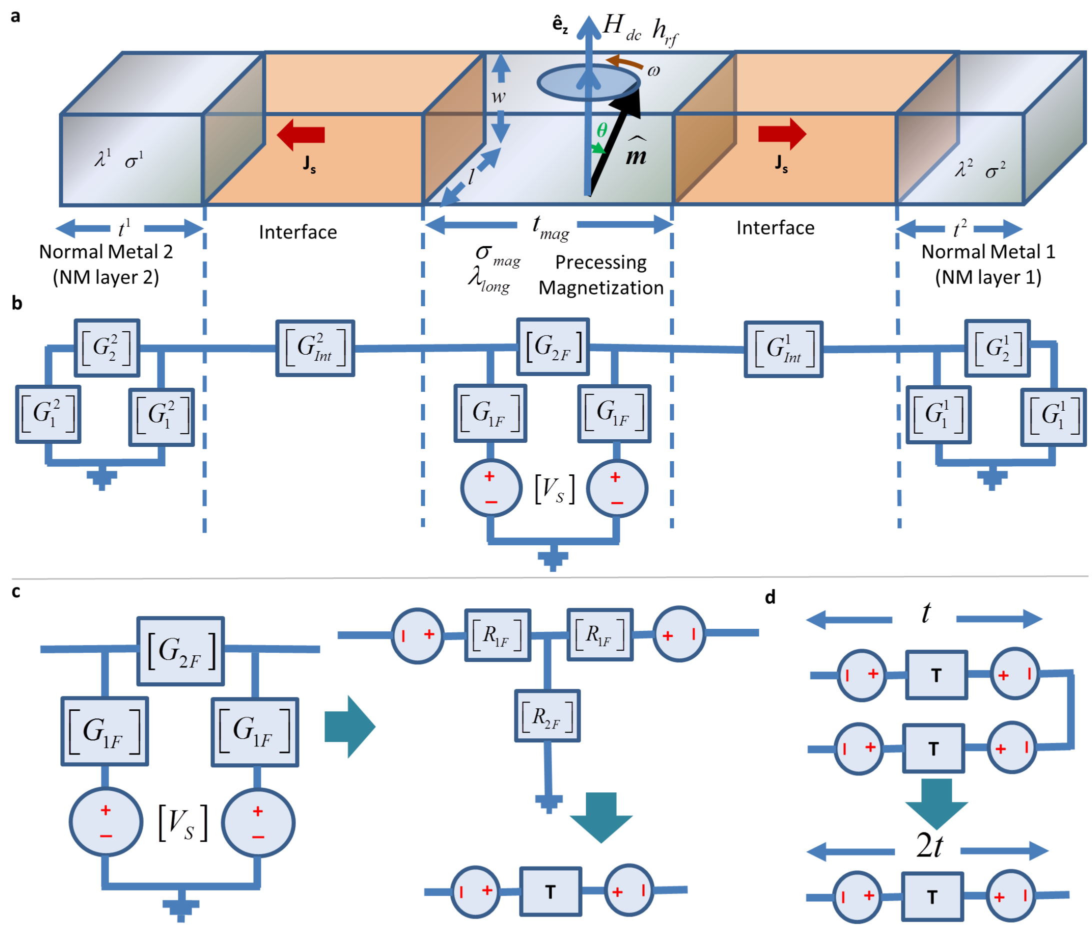

FIG. 1. (a) A precessing magnetization in a magnetic layer with uniform mode of excitation. This can generate a pure spin current to the adjacent normal metals (NMs). J_s is the spin current density, H_{dc} is the applied dc magnetic field, h_{rf} is the rf driving field, ω and θ are the precession frequency and angle, respectively. (b) Spin circuit representation of spin pumping for ferromagnet (FM), NM, and FM-NM interface. The voltage source $[V_S]$ acts as a spin battery, $[G_{Int}^{1(2)}]$ is the FM-NM interfacial spin mixing conductances for the two interfaces. (c) The FM π-circuit can be converted to an equivalent T-circuit. (d) Two T-circuits can be joined to get an equivalent T-circuit of twice length. Note that the voltage sources in between the two T-circuits get canceled out and thus the spin battery only appears at the interfaces.

$$\left[G_1^{1(2)}\right] = \begin{pmatrix} 0 & 0 & 0 & 0 \\ 0 & G_{1n}^{1(2)} & 0 & 0 \\ 0 & 0 & G_{1n}^{1(2)} & 0 \\ 0 & 0 & 0 & G_{1n}^{1(2)} \end{pmatrix}, \tag{3}$$

$$\left[G_2^{1(2)}\right] = \begin{pmatrix} G_n^{1(2)} & 0 & 0 & 0 \\ 0 & G_{2n}^{1(2)} & 0 & 0 \\ 0 & 0 & G_{2n}^{1(2)} & 0 \\ 0 & 0 & 0 & G_{2n}^{1(2)} \end{pmatrix}, \tag{4}$$

$$[G_{1F}] = \begin{pmatrix} 0 & 0 & 0 & 0 \\ 0 & G_{sh}^z & 0 & 0 \\ 0 & 0 & \infty & \infty \\ 0 & 0 & \infty & \infty \end{pmatrix}, [G_{2F}] = \begin{pmatrix} G_f & PG_f & 0 & 0 \\ PG_f & G_{se}^z & 0 & 0 \\ 0 & 0 & 0 & 0 \\ 0 & 0 & 0 & 0 \end{pmatrix}, \tag{5}$$

$$\left[G_{Int}^{1(2)}\right] = \begin{pmatrix} G_I^{1(2)} & P_I^{1(2)}G_I^{1(2)} & 0 & 0 \\ P_I^{1(2)}G_I^{1(2)} & G_I^{1(2)} & 0 & 0 \\ 0 & 0 & 2G_r^{\uparrow\downarrow 1(2)} & 2G_i^{\uparrow\downarrow 1(2)} \\ 0 & 0 & 2G_i^{\uparrow\downarrow 1(2)} & 2G_r^{\uparrow\downarrow 1(2)} \end{pmatrix}, \tag{6}$$

and $[V_S] = \begin{bmatrix} 0 & \vec{V}_{SP} \end{bmatrix}^T$,

where $G_f = \sigma_{mag} lw/t_{mag}$, $G_n^{1(2)} = \sigma^{1(2)} lw/t^{1(2)}$, $G_z = \sigma_z lw/t_{mag}$, $G_{sh}^z = G_z Q\, tanh(t_{mag}/2\lambda_{long})$, $G_{se}^z = G_z \left(P^2 + Q\, csch(t_{mag}/2\lambda_{long})\right)$, $Q = (t_{mag}/\lambda_{long})(1 - P^2)$, $G_{1n}^{1(2)} = (\sigma^{1(2)} lw/t^{1(2)}) tanh(t^{1(2)}/2\lambda^{1(2)})$, $G_{2n}^{1(2)} = (\sigma^{1(2)} lw/t^{1(2)}) csch(t/\lambda^{1(2)})$,
P is the spin polarization of the FM, G_I and P_I are the FM-NM interface conductance and polarization, respectively, $\lambda^{1(2)}$, $\sigma^{1(2)}$, and $t^{1(2)}$ are the spin diffusion length, conductivity, and thickness of the $\mathrm{NM}^{1(2)}$ layer, respectively, λ_{long}, σ_z, and t_{mag} are the *longitudinal* spin

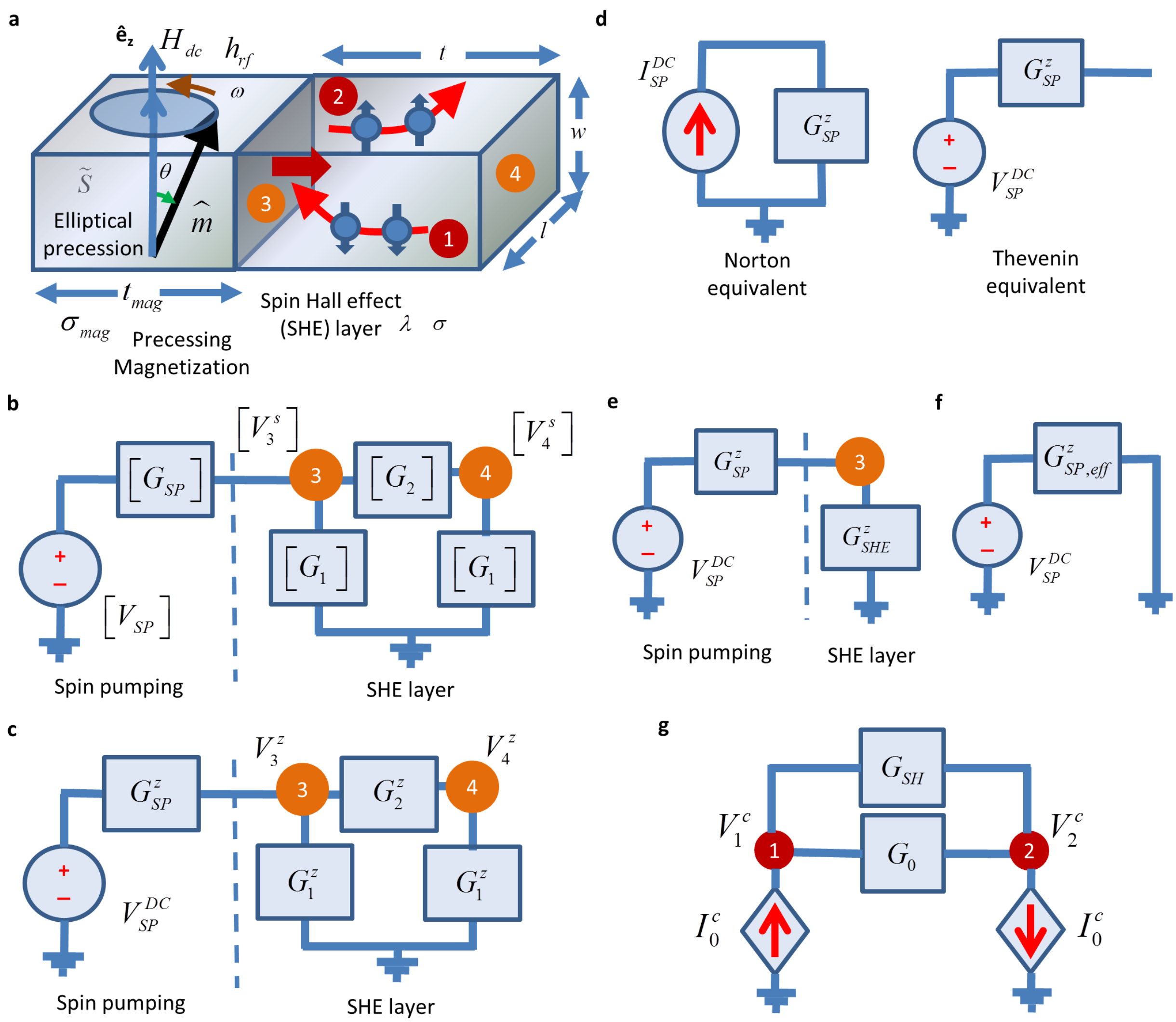

FIG. 2. (a) A precessing magnetization is pumping pure spin current to an adjacent layer possessing a high spin orbit coupling and it generates a considerable amount of charge current due to inverse spin Hall effect (ISHE). Charge potentials are developed at the surfaces marked by 1 and 2, while spin potentials are developed at the surfaces marked by 3 and 4. (b) Instantaneous 3-component spin circuit with the voltage source $[V_{SP}]$ acts as a spin battery, $[G_{SP}]$ is the interfacial spin mixing conductance between the magnetic layer and the SHE layer. (c) A dc spin circuit with average spin polarization acting in the z-direction. (d) The spin circuit for the spin pumping can be represented by either Thevenin-equivalent with a spin battery or Norton-equivalent with a spin current source. (e) Reduced spin circuit with the SHE layer conductance represented by a single conductance. (f) Spin circuit representing the effective spin mixing conductance with the SHE layer conductance included in it. (g) The charge circuit for the spin-to-charge conversion by ISHE with the current sources I_0^c dependent on the spin circuit in the part (c), G_0 and G_{SH} are the conductances for the SHE and FM layers, respectively.

diffusion length, conductivity, and thickness of the FM layer, respectively, and $l \times w$ is the cross-sectional area.

The following points should be noted from the spin circuit representation of spin pumping in the Fig. 1: (1) We include the spin battery in the FM module since a magnet can be precessed without the connection of an NM module. (2) Figs. 1(c) and 1(d) explain (see the caption) that the spin battery appears at the interface only, which accords with the established physical concept in literature [5]. (3) We consider the transverse components $(x-y)$ of the conductances entirely at the FM-NM interface ($[G_{int}^{1(2)}]$), thus the transverse components of $[G_{1F}]$ are ∞. (4) We consider that the magnet is thick enough (compared to the *transverse* spin diffusion length λ_{tran}, which is a few monolayers for the typical transition metals) so that the *transmission* spin mixing conductances are nearly zero, and thus we only consider the *reflection* spin mixing conductances [5]. (5) For magnetic insulators [39], $\sigma_{mag} = 0$, $P = 0$, σ_z (λ_{long}) represents the spin wave/magnon conductivity (diffusion length), and the *transmission* spin mixing conductances are *exactly* zero (i.e., the transverse components of $[G_{1F}]$ and $[G_{2F}]$ are *exactly* ∞ and 0, respectively).

Figure 2 shows the 3-component version of spin pumping and the generation of inverse spin Hall voltage in the transverse direction due to the symmetry involved in the system [14]. The instantaneous spin pumping [Figure 2(b)] in matrix form can be represented by $[I_{SP}] = [G_{SP}]\,[V_{SP}]$, where

$$[I_{SP}] = lw\,\tilde{S}\,\left(\frac{2e}{\hbar}\right)\frac{\hbar\omega}{4\pi}\begin{pmatrix} g_r^{\uparrow\downarrow}\left(1-m_z^2\right) \\ -g_r^{\uparrow\downarrow}m_xm_z - g_i^{\uparrow\downarrow}m_y \\ -g_r^{\uparrow\downarrow}m_ym_z + g_i^{\uparrow\downarrow}m_x \end{pmatrix}, \quad (7)$$

$$[V_{SP}] = \tilde{S}\,\frac{\hbar\omega}{2e}\begin{pmatrix} \left(1-m_z^2\right) \\ -m_xm_z \\ -m_ym_z \end{pmatrix}, \quad (8)$$

$G_r^{\uparrow\downarrow} = lw\,(e^2/h)\,g_r^{\uparrow\downarrow}$, $G_i^{\uparrow\downarrow} = lw\,(e^2/h)\,g_i^{\uparrow\downarrow}$ ($g^{\uparrow\downarrow} = g_r^{\uparrow\downarrow} + ig_i^{\uparrow\downarrow}$ is the complex spin mixing conductance per unit area), $\tilde{S}$ is the frequency dependent elliptical precession factor due to thin magnetic film [40], the components of $[G_{SP}]$

$$\begin{aligned} G_{SP}^{nn} &= 2G_r^{\uparrow\downarrow}\left(1-m_n^2\right) \quad n=(x,y,z), \\ G_{SP}^{xy}(G_{SP}^{yx}) &= -2G_r^{\uparrow\downarrow}m_xm_z \pm 2G_i^{\uparrow\downarrow}m_y, \\ G_{SP}^{yz}(G_{SP}^{zy}) &= -2G_r^{\uparrow\downarrow}m_xm_y \pm 2G_i^{\uparrow\downarrow}m_z, \\ G_{SP}^{zx}(G_{SP}^{xz}) &= -2G_r^{\uparrow\downarrow}m_ym_z \pm 2G_i^{\uparrow\downarrow}m_x, \end{aligned}$$

$[G_1] = G_\lambda tanh\left(\frac{t}{2\lambda}\right)[I_{3\times3}]$, $[G_2] = G_\lambda csch\left(\frac{t}{\lambda}\right)[I_{3\times3}]$, $G_\lambda = \sigma lw/\lambda$, and $[I_{3\times3}]$ is the 3×3 identity matrix.

The spin circuit representation of average spin pumping for a complete precession is depicted in the Fig. 2(c) with the voltage source (or the current source depicted in the Fig. 2(d)) represented by $V_{SP}^{DC} = \tilde{S}\,\frac{\hbar\omega}{2e}sin^2\theta$ ($I_{SP}^{DC} = lw\,\tilde{S}\,\frac{e\omega}{2\pi}g_r^{\uparrow\downarrow}sin^2\theta$). Thus $G_{SP}^z = I_{SP}^{DC}/V_{SP}^{DC} = lw(2e^2/h)g_r^{\uparrow\downarrow}$. Note that first principles calculations and experiments have shown that the imaginary component of $g^{\uparrow\downarrow}$ is negligible for metallic interfaces (i.e., $g^{\uparrow\downarrow} \simeq g_r^{\uparrow\downarrow}$) [14, 27]. $G_1^z = G_\lambda tanh(t/2\lambda)$, $G_2^z = G_\lambda csch(t/\lambda)$. From Fig. 2(d), $G_{SHE}^z = G_1^z + G_1^zG_2^z/(G_1^z + G_2^z) = G_\lambda/coth(t/\lambda)$. From Fig. 2(e), we get $G_{SP,eff}^z = G_{SP}^zG_{SHE}^z/(G_{SP}^z + G_{SHE}^z) = lw(2e^2/h)g_{eff}^{\uparrow\downarrow}$. Hence, we get

$$g_{eff}^{\uparrow\downarrow} = \frac{g^{\uparrow\downarrow}}{1+\frac{\lambda}{\sigma}\,\frac{2e^2}{h}g^{\uparrow\downarrow}coth\left(\frac{t}{\lambda}\right)}, \quad (9)$$

which matches the mathematical expression derived in literature [5]. The above equation can be backcalculated to get the the bare spin mixing conductance $g^{\uparrow\downarrow}$ with the inequality $(2e^2\lambda/h\sigma)g_{eff}^{\uparrow\downarrow}\,coth(t/\lambda) < 1$, since $g^{\uparrow\downarrow} > 0$. Note that $g_{eff}^{\uparrow\downarrow}$ (and not the bare $g^{\uparrow\downarrow}$) can be determined from the enhancement of damping in ferromagnetic resonance experiments [14].

Figure 2(g) shows the charge circuit for the generation of inverse spin Hall voltage [36] ($V_{ISHE} = V_2^c - V_1^c$), which also considers the conductance $G_{SH} = \sigma_{mag}t_{mag}w/l$ due to current shunting through the magnet, if it is metallic. The charge current sources in Fig. 2(g), depend on the spin potential difference between the nodes 3 and 4 in the Fig. 2(c) as $I_0^c = \beta G_0\,(V_3^z - V_4^z)$, where $G_0 = \sigma tw/l$, $\beta = \theta_{sh}l/t$, and θ_{sh} is the spin Hall angle [36].

Applying KCL at node 1 of the charge circuit in Fig. 2(g), we get $I_0^c = (V_1^c - V_2^c)\,(G_0 + G_{SH})$ and hence

$$V_{ISHE} = -\beta\left(\frac{G_0}{G_0+G_{SH}}\right)(V_3^z - V_4^z)\,. \quad (10)$$

To calculate $(V_3^z - V_4^z)$, we apply KCL at nodes 3 and 4 of the spin circuit in Fig. 2(c), and we get

$$\begin{aligned} \left(V_3^z - V_{SP}^{DC}\right)G_{SP}^z + V_3^zG_1^z + (V_3^z - V_4^z)\,G_2^z &= 0, \quad (11) \\ V_4^zG_1^z + (V_4^z - V_3^z)\,G_2^z &= 0. \quad (12) \end{aligned}$$

After solving, we get

$$V_3^z = \frac{G_1^z + G_2^z}{D}V_{SP}^{DC}G_{SP}^z, \quad V_4^z = \frac{G_2^z}{D}V_{SP}^{DC}G_{SP}^z, \quad (13)$$

where $D = (G_1^z + G_2^z)\,(G_{SP}^z + G_1^z + G_2^z) - (G_2^z)^2$. From Equation (10), we get

$$V_{ISHE} = -\frac{\theta_{SH}l\lambda e\tilde{S}\omega g^{\uparrow\downarrow}sin^2\theta tanh\left(\frac{t}{2\lambda}\right)}{2\pi\left(\sigma t + \sigma_{mag}t_{maag}\right)\left(1+\frac{\lambda}{\sigma}\,\frac{2e^2}{h}g^{\uparrow\downarrow}coth\left(\frac{t}{\lambda}\right)\right)}, \quad (14)$$

which matches the mathematical expression derived in literature [14].

We further study the spin pumping in two subsequent NM layers [38] using spin circuit. We deduce the expression for the spin conductance of the two layers G_L by simply reducing the spin circuit (see Supplementary Fig. S1 and the detailed derivation [37]) and show that it matches the mathematical expression derived in Ref. [38]. We can simply write a netlist containing the conductances and voltage/current sources to determine the effective spin mixing conductance of the whole structure $G_{SP,eff}$ [37]. For more complex structures, the analytical expression becomes tedious and this establishes that the spin circuit approach presented here is a versatile and effective tool for analyzing and proposing functional spintronic devices. Also note that the 3-component circuit in Fig. 2(b) and and the 4-component circuit in Fig. 1 can be solved in general.

To summarize, we have developed the spin circuit representation of spin pumping and have shown that such representation accords to the established mathematical expressions in literature. Such circuits can be simply solved analytically and when more complex they can be solved programmatically to analyze and propose complex devices. We have not considered conductance for the interfacial Rashba-Edelstein effect at NM-NM interface [41] or any significant interfacial spin memory loss at FM-NM interface, on which (and also on spin diffusion length, spin Hall angle) there is controversy [42]. It needs to also carefully consider the low-thickness regime and the effect of magnetic proximity effect [43]. The spin circuit presented here has immense consequence on the development of spintronic technology.

This work was supported by FAME, one of six centers of STARnet, a Semiconductor Research Corporation program sponsored by MARCO and DARPA.

[1] L. Onsager, Reciprocal relations in irreversible processes. I., Phys. Rev. **37**, 405 (1931); Reciprocal relations in irreversible processes. II., **38**, 2265 (1931).

[2] R. H. Silsbee, A. Janossy, and P. Monod, Coupling between ferromagnetic and conduction-spin-resonance modes at a ferromagnetic–normal-metal interface, Phys. Rev. B **19**, 4382 (1979).

[3] S. Mizukami, Y. Ando, and T. Miyazaki, Ferromagnetic resonance linewidth for NM/80NiFe/NM films (NM= Cu, Ta, Pd and Pt), J. Magn. Magn. Mater. **226**, 1640 (2001); The study on ferromagnetic resonance linewidth for NM/80NiFe/NM (NM= Cu, Ta, Pd and Pt) films, Jap. J. Appl. Phys. **40**, 580 (2001); Effect of spin diffusion on Gilbert damping for a very thin permalloy layer in Cu/permalloy/Cu/Pt films, Phys. Rev. B **66**, 104413 (2002); Magnetic relaxation of normal-metal (NM)/80NiFe/NM films, J. Magn. Magn. Mater. **239**, 42 (2002); B. Heinrich, K. B. Urquhart, A. S. Arrott, J. F. Cochran, K. Myrtle, and S. T. Purcell, Ferromagnetic-resonance study of ultrathin bcc Fe (100) films grown epitaxially on fcc Ag (100) substrates, Phys. Rev. Lett. **59**, 1756 (1987); R. Urban, G. Woltersdorf, and B. Heinrich, Gilbert damping in single and multilayer ultrathin films: role of interfaces in nonlocal spin dynamics, **87**, 217204 (2001); W. Platow, A. N. Anisimov, G. L. Dunifer, M. Farle, and K. Baberschke, Correlations between ferromagnetic-resonance linewidths and sample quality in the study of metallic ultrathin films, Phys. Rev. B **58**, 5611 (1998).

[4] Y. Tserkovnyak, A. Brataas, and G. E. W. Bauer, Enhanced Gilbert damping in thin ferromagnetic films, Phys. Rev. Lett. **88**, 117601 (2002); Spin pumping and magnetization dynamics in metallic multilayers, Phys. Rev. B **66**, 224403 (2002).

[5] Y. Tserkovnyak, A. Brataas, G. E. W. Bauer, and B. I. Halperin, Nonlocal magnetization dynamics in ferromagnetic heterostructures, Rev. Mod. Phys. **77**, 1375 (2005).

[6] M. V. Costache, M. Sladkov, S. M. Watts, C. H. van der Wal, and B. J. van Wees, Electrical detection of spin pumping due to the precessing magnetization of a single ferromagnet, Phys. Rev. Lett. **97**, 216603 (2006).

[7] K. Ando, S. Takahashi, J. Ieda, H. Kurebayashi, T. Trypiniotis, C. H. W. Barnes, S. Maekawa, and E. Saitoh, Electrically tunable spin injector free from the impedance mismatch problem, Nature Mater. **10**, 655 (2011).

[8] A. Brataas, Y. Tserkovnyak, G. E. W. Bauer, and P. J. Kelly, Spin pumping and spin transfer, in *Spin Current*, Vol. 17, edited by S. Maekawa, S. O. Valenzuela, E. Saitoh, and T. Kimura (Oxford University Press, 2012) pp. 87–135.

[9] J. C. Slonczewski, Current-driven excitation of magnetic multilayers, J. Magn. Magn. Mater. **159**, L1 (1996); L. Berger, Emission of spin waves by a magnetic multilayer traversed by a current, Phys. Rev. B **54**, 9353 (1996); J. Z. Sun, Spin-current interaction with a monodomain magnetic body: A model study, **62**, 570 (2000); M. D. Stiles and A. Zangwill, Anatomy of spin-transfer torque, **66**, 14407 (2002).

[10] P. W. Brouwer, Scattering approach to parametric pumping, Phys. Rev. B **58**, R10135 (1998); M. Büttiker, H. Thomas, and A. Prêtre, Current partition in multiprobe conductors in the presence of slowly oscillating external potentials, Z. Phys. B **94**, 133 (1994).

[11] Y. Guan, W. E. Bailey, E. Vescovo, C.-C. Kao, and D. A. Arena, Phase and amplitude of element-specific moment precession in $Ni_{81}Fe_{19}$, J. Magn. Magn. Mater. **312**, 374 (2007).

[12] T. Kimura, Y. Otani, T. Sato, S. Takahashi, and S. Maekawa, Room-temperature reversible spin Hall effect, Phys. Rev. Lett. **98**, 156601 (2007).

[13] K. Ando, S. Takahashi, K. Harii, K. Sasage, J. Ieda, S. Maekawa, and E. Saitoh, Electric manipulation of spin relaxation using the spin Hall effect, Phys. Rev. Lett. **101**, 036601 (2008).

[14] O. Mosendz, J. E. Pearson, F. Y. Fradin, G. E. W. Bauer, S. D. Bader, and A. Hoffmann, Quantifying spin Hall angles from spin pumping: Experiments and theory, Phys. Rev. Lett. **104**, 046601 (2010); O. Mosendz, V. Vlaminck, J. E. Pearson, F. Y. Fradin, G. E. W. Bauer, S. D. Bader, and A. Hoffmann, Detection and quantification of inverse spin Hall effect from spin pumping in permalloy/normal metal bilayers, Phys. Rev. B **82**, 214403 (2010).

[15] L. Liu, T. Moriyama, D. C. Ralph, and R. A. Buhrman, Spin-torque ferromagnetic resonance induced by the spin Hall effect, Phys. Rev. Lett. **106**, 036601 (2011); L. Liu, C. F. Pai, Y. Li, H. W. Tseng, D. C. Ralph, and R. A. Buhrman, Spin-torque switching with the giant spin Hall effect of tantalum, Science **336**, 555 (2012); C. F. Pai, L. Liu, Y. Li, H. W. Tseng, D. C. Ralph, and R. A. Buhrman, Spin transfer torque devices utilizing the giant spin Hall effect of tungsten, Appl. Phys. Lett. **101**, 122404 (2012); Y. Niimi, M. Morota, D. H. Wei, C. Deranlot, M. Basletic, A. Hamzic, A. Fert, and Y. Otani, Extrinsic spin Hall effect induced by iridium impurities in copper, Phys. Rev. Lett. **106**, 126601 (2011); Y. Niimi, Y. Kawanishi, D. H. Wei, C. Deranlot, H. X. Yang, M. Chshiev, T. Valet, A. Fert, and Y. Otani, Giant Spin Hall Effect Induced by Skew Scattering from Bismuth Impurities inside Thin Film CuBi Alloys, **109**, 156602 (2012); Y. Niimi, H. Suzuki, Y. Kawanishi, Y. Omori, T. Valet, A. Fert, and Y. Otani, Extrinsic spin Hall effects measured with lateral spin valve structures, Phys. Rev. B **89**, 054401 (2014); P. Laczkowski, J. C. Rojas-Sánchez, W. Savero-Torres, H. Jaffrès, N. Reyren, C. Deranlot, L. Notin, C. Beigné, A. Marty, and J. P. Attané, Experimental evidences of a large extrinsic spin Hall effect in AuW alloy, Appl. Phys. Lett. **104**, 142403 (2014).

[16] X. Wang, G. E. W. Bauer, B. J. van Wees, A. Brataas, and Y. Tserkovnyak, Voltage generation by ferromagnetic resonance at a nonmagnet to ferromagnet contact, Phys. Rev. Lett. **97**, 216602 (2006).

[17] H. Jiao and G. E. W. Bauer, Spin backflow and ac voltage generation by spin pumping and the inverse spin Hall effect, Phys. Rev. Lett. **110**, 217602 (2013).

[18] A. Azevedo, L. H. Vilela-Leão, R. L. Rodríguez-Suárez, A. B. Oliveira, and S. M. Rezende, dc effect in ferromagnetic resonance: Evidence of the spin-pumping effect? J. Appl. Phys. **97**, 10C715 (2005).

[19] E. Saitoh, M. Ueda, H. Miyajima, and G. Tatara, Conversion of spin current into charge current at room temperature: Inverse spin-Hall effect, Appl. Phys. Lett. **88**, 182509 (2006).

[20] M. I. Dyakonov and V. I. Perel, Possibility of orienting

electron spins with current, Sov. Phys. JETP Lett. **13**, 467 (1971); J. E. Hirsch, Spin Hall effect, Phys. Rev. Lett. **83**, 1834 (1999); S. Zhang, Spin Hall effect in the presence of spin diffusion, **85**, 393 (2000).

[21] S. Murakami, N. Nagaosa, and S. C. Zhang, Dissipationless quantum spin current at room temperature, Science **301**, 1348 (2003); J. Sinova, D. Culcer, Q. Niu, N. A. Sinitsyn, T. Jungwirth, and A. H. MacDonald, Universal intrinsic spin Hall effect, Phys. Rev. Lett. **92**, 126603 (2004); J. Sinova, S. O. Valenzuela, J. Wunderlich, C. H. Back, and T. Jungwirth, Spin Hall effects, Rev. Mod. Phys. **87**, 1213 (2015).

[22] S. O. Valenzuela and M. Tinkham, Direct electronic measurement of the spin Hall effect, Nature **442**, 176 (2006).

[23] K. Roy, Ultra-low-energy computing paradigm using giant spin Hall devices, J. Phys. D: Appl. Phys. **47**, 422001 (2014).

[24] A. Brataas, Y. Tserkovnyak, G. E. W. Bauer, and B. I. Halperin, Spin battery operated by ferromagnetic resonance, Phys. Rev. B **66**, 060404 (2002).

[25] A. Brataas, G. E. W. Bauer, and P. J. Kelly, Noncollinear magnetoelectronics, Phys. Rep. **427**, 157–255 (2006).

[26] A. Brataas, Y. V. Nazarov, and G. E. W. Bauer, Finite-element theory of transport in ferromagnet-normal metal systems, Phys. Rev. Lett. **84**, 2481 (2000); Spin-transport in multi-terminal normal metal-ferromagnet systems with non-collinear magnetizations, Eur. Phys. J. B **22**, 99 (2001).

[27] M. Zwierzycki, Y. Tserkovnyak, P. J. Kelly, A. Brataas, and G. E. W. Bauer, First-principles study of magnetization relaxation enhancement and spin transfer in thin magnetic films, Phys. Rev. B **71**, 064420 (2005).

[28] M. Weiler, M. Althammer, M. Schreier, J. Lotze, M. Pernpeintner, S. Meyer, H. Huebl, R. Gross, A. Kamra, J. Xiao, Y. T. Chen, H. Jiao, G. E. W. Bauer, and S. T. B. Goennenwein, Experimental test of the spin mixing interface conductivity concept, Phys. Rev. Lett. **111**, 176601 (2013).

[29] Y. Imry and R. Landauer, Conductance viewed as transmission, Rev. Mod. Phys. **71**, S306 (1999); R. Landauer, Spatial variation of currents and fields due to localized scatterers in metallic conduction, IBM J. Res. Dev. **1**, 223–231 (1957); M. Buttiker, Symmetry of electrical conduction, **32**, 317 (1988).

[30] L. Landau and E. Lifshitz, On the theory of the dispersion of magnetic permeability in ferromagnetic bodies, Phys. Z. Sowjet. **8**, 153 (1935); T. L. Gilbert, A phenomenological theory of damping in ferromagnetic materials, IEEE Trans. Magn. **40**, 3443 (2004).

[31] V. Kamberský, Spin-orbital Gilbert damping in common magnetic metals, Phys. Rev. B **76**, 134416 (2007).

[32] *HSPICE, Circuit simulation software*, Synopsys, www.synopsys.com.

[33] J. M. Rabaey, A. P. Chandrakasan, and B. Nikoliç, *Digital Integrated Circuits* (Pearson Education, 2003).

[34] C.-T. Sah, Equivalent Circuit Models in Semiconductor Transport for Thermal, Optical, Auger-Impact, and Tunnelling Recombination–Generation–Trapping Processes, physica status solidi (a) **7**, 541 (1971).

[35] S. Srinivasan, V. Diep, B. Behin-Aein, A. Sarkar, and S. Datta, Modeling multi-magnet networks interacting via spin currents, in *Handbook of Spintronics*, edited by Yongbing Xu, D. David Awschalom, and Junsaku Nitta (Springer Netherlands, Dordrecht, 2014) pp. 1–49.

[36] S. Hong, S. Sayed, and S. Datta, Spin circuit representation for the spin Hall effect, IEEE Trans. Nanotech. **15**, 225 (2016).

[37] See supplementary material at .... for additional detailed derivation for spin pumping in multilayers.

[38] K. Harii, Z. Qiu, T. Iwashita, Y. Kajiwara, K. Uchida, K. Ando, T. An, Y. Fujikawa, and E. Saitoh, Spin pumping in a ferromagnetic/nonmagnetic/spin-sink trilayer film: spin current termination, Key Eng. Mater. **508**, 266 (2012).

[39] Y. Kajiwara, K. Harii, S. Takahashi, J. Ohe, K. Uchida, M. Mizuguchi, H. Umezawa, H. Kawai, K. Ando, and K. Takanashi, Transmission of electrical signals by spin-wave interconversion in a magnetic insulator, Nature **464**, 262 (2010); B. Heinrich, C. Burrowes, E. Montoya, B. Kardasz, E. Girt, Y. Y. Song, Y. Sun, and M. Wu, Spin pumping at the magnetic insulator (YIG)/normal metal (Au) interfaces, Phys. Rev. Lett. **107**, 066604 (2011); V. Castel, N. Vlietstra, J. B. Youssef, and B. J. van Wees, Platinum thickness dependence of the inverse spin-Hall voltage from spin pumping in a hybrid yttrium iron garnet/platinum system, Appl. Phys. Lett. **101**, 132414 (2012); A. Kapelrud and A. Brataas, Spin pumping and enhanced Gilbert damping in thin magnetic insulator films, Phys. Rev. Lett. **111**, 097602 (2013); Y. Sun, H. Chang, M. Kabatek, Y. Y. Song, Z. Wang, M. Jantz, W. Schneider, M. Wu, E. Montoya, B. Kardasz, B. Heinrich, S. G. E. te Velthuis, Schultheiss H., and A. Hoffmann, Damping in yttrium iron garnet nanoscale films capped by platinum, **111**, 106601 (2013); Y. Zhou, H. Jiao, Y. Chen, G. E. W. Bauer, and J. Xiao, Current-induced spin-wave excitation in Pt/YIG bilayer, Phys. Rev. B **88**, 184403 (2013); H. L. Wang, C. H. Du, Y. Pu, R. Adur, P. C. Hammel, and F. Y. Yang, Scaling of Spin Hall Angle in 3d, 4d, and 5d Metals from $Y_3Fe_5O_{12}$/Metal Spin Pumping, Phys. Rev. Lett. **112**, 197201 (2014).

[40] K. Ando, T. Yoshino, and E. Saitoh, Optimum condition for spin-current generation from magnetization precession in thin film systems, Appl. Phys. Lett. **94**, 152509 (2009).

[41] V. M. Edelstein, Spin polarization of conduction electrons induced by electric current in two-dimensional asymmetric electron systems, Solid State Commun. **73**, 233 (1990); J. C. Rojas Sánchez, L. Vila, G. Desfonds, S. Gambarelli, J. P. Attané, J. M. De Teresa, C. Magén, and A. Fert, Spin-to-charge conversion using Rashba coupling at the interface between non-magnetic materials, Nature Commun. **4**, 2944 (2013); W. Zhang, M. B. Jungfleisch, W. Jiang, J. E. Pearson, and A. Hoffmann, Spin pumping and inverse Rashba-Edelstein effect in NiFe/Ag/Bi and NiFe/Ag/Sb, J. Appl. Phys. **117**, 17C727 (2015).

[42] A. Fert and S. F. Lee, Theory of the bipolar spin switch, Phys. Rev. B **53**, 6554 (1996); A. A. Kovalev, A. Brataas, and G. E. W. Bauer, Spin transfer in diffusive ferromagnet-normal metal systems with spin-flip scattering, **66**, 224424 (2002); H. Y. T. Nguyen, W. P. Pratt, and J. Bass, Spin-flipping in Pt and at Co/Pt interfaces, J. Magn. Magn. Mater. **361**, 30 (2014); Z. Feng, J. Hu, L. Sun, B. You, D. Wu, J. Du, W. Zhang, A. Hu, Y. Yang, and D. M. Tang, Spin Hall angle quantification from spin pumping and microwave photoresistance, Phys. Rev. B **85**, 214423 (2012); J. C. Rojas-Sánchez, N. Reyren, P. Laczkowski, W. Savero, J. P. Attané,

C. Deranlot, M. Jamet, J. M. George, L. Vila, and H. Jaffrès, Spin Pumping and Inverse Spin Hall Effect in Platinum: The Essential Role of Spin-Memory Loss at Metallic Interfaces, Phys. Rev. Lett. **112**, 106602 (2014); Y. Liu, Z. Yuan, R. J. H. Wesselink, A. A. Starikov, and P. J. Kelly, Interface enhancement of Gilbert damping from first principles, **113**, 207202 (2014); K. Chen and S. Zhang, Spin pumping in the presence of spin-orbit coupling, **114**, 126602 (2015); W. Zhang, W. Han, X. Jiang, S. H. Yang, and S. S. P. Parkin, Role of transparency of platinum-ferromagnet interfaces in determining the intrinsic magnitude of the spin Hall effect, Nature Phys. **11**, 496 (2015); W. Zhang, V. Vlaminck, J. E. Pearson, R. Divan, S. D. Bader, and A. Hoffmann, Determination of the Pt spin diffusion length by spin-pumping and spin Hall effect, Appl. Phys. Lett. **103**, 242414 (2013); C. T. Boone, J. M. Shaw, H. T. Nembach, and T. J. Silva, Spin-scattering rates in metallic thin films measured by ferromagnetic resonance damping enhanced by spin-pumping, J. Appl. Phys. **117**, 223910 (2015).

[43] S. Y. Huang, X. Fan, D. Qu, Y. P. Chen, W. G. Wang, J. Wu, T. Y. Chen, J. Q. Xiao, and C. L. Chien, Transport magnetic proximity effects in platinum, Phys. Rev. Lett. **109**, 107204 (2012); Y. M. Lu, Y. Choi, C. M. Ortega, X. M. Cheng, J. W. Cai, S. Y. Huang, L. Sun, and C. L. Chien, Pt magnetic polarization on $Y_3Fe_5O_{12}$ and magnetotransport characteristics, **110**, 147207 (2013); W. L. Lim, N. Ebrahim-Zadeh, J. C. Owens, H. G. E. Hentschel, and S. Urazhdin, Temperature-dependent proximity magnetism in Pt, Appl. Phys. Lett. **102**, 162404 (2013); Y. Yang, B. Wu, K. Yao, S. Shannigrahi, B. Zong, and Y. Wu, Investigation of magnetic proximity effect in Ta/YIG bilayer Hall bar structure, J. Appl. Phys. **115**, 17C509 (2014); W. Zhang, M. B. Jungfleisch, W. Jiang, Y. Liu, J. E. Pearson, S. G. E. te Velthuis, A. Hoffmann, F. Freimuth, and Y. Mokrousov, Reduced spin-Hall effects from magnetic proximity, Phys. Rev. B **91**, 115316 (2015); M. Caminale, A. Ghosh, S. Auffret, U. Ebels, K. Ollefs, F. Wilhelm, A. Rogalev, and W. E. Bailey, Spin pumping damping and magnetic proximity effect in Pd and Pt spin-sink layers, **94**, 014414 (2016).